Article

Catalytic Transesterification of Dialkyl Phosphates by a Bioinspired Dicopper(II) Macrocyclic Complex

Malgorzata Jagoda, Sabine Warzeska, Hans Pritzkow, Hubert Wadepohl, Petra Imhof, Jeremy C. Smith, and Roland Krmer

J. Am. Chem. Soc., **2005**, 127 (43), 15061-15070• DOI: 10.1021/ja051357b • Publication Date (Web): 06 October 2005

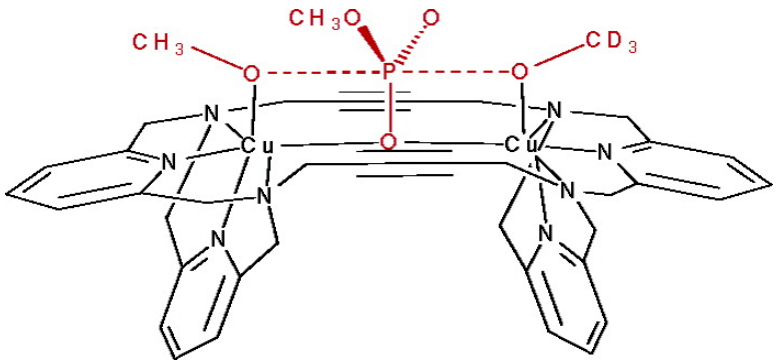

More About This Article

Additional resources and features associated with this article are available within the HTML version:

- Supporting Information
- Links to the 6 articles that cite this article, as of the time of this article download
- Access to high resolution figures
- Links to articles and content related to this article
- Copyright permission to reproduce figures and/or text from this article

View the Full Text HTML

J|A|C|S
ARTICLES
Published on Web 10/06/2005

Catalytic Transesterification of Dialkyl Phosphates by a Bioinspired Dicopper(II) Macrocyclic Complex

Malgorzata Jagoda,[†] Sabine Warzeska,[†] Hans Pritzkow,[†] Hubert Wadepohl,[†] Petra Imhof,[‡] Jeremy C. Smith,[‡] and Roland Krämer*[,†]

Contribution from the Universität Heidelberg, Anorganisch-Chemisches Institut, Im Neuenheimer Feld 270, 69120 Heidelberg, Germany, and Universität Heidelberg, IWR, Uni-Heidelberg, Im Neuenheimer Feld 368, 69120 Heidelberg, Germany

Received March 3, 2005; E-mail: roland.kraemer@urz.uni-heidelberg.de

Abstract: For a number of phosphoryltransfer enzymes, including the exonuclease subunit of DNA polymerase I, a mechanism involving two-metal ions and double Lewis-acid activation of the substrate, combined with leaving group stabilization, has been proposed. Inspired by the active site structure of this enzyme, we have designed as a synthetic phosphoryl transfer catalyst the dicopper(II) macrocyclic complex **LCu$_2$**. Crystal structures of complexes [(**L**)Cu$_2$(μ-NO$_3$)(NO$_3$)](NO$_3$)$_2$ (**1**), [(**L**)Cu$_2$(μ-CO$_3$)(CH$_3$OH)](BF$_4$)$_2$ (**2**), and [(**L**)Cu$_2$(μ-O$_2$P(OCH$_3$)$_2$)(NO$_3$)](NO$_3$)$_2$ (**3**) illustrate various possibilities for the interaction of oxoanions with the dicopper(II) site. **1** efficiently promotes the transesterification of dimethyl phosphate (DMP) in CD$_3$OD, $k_{cat} = 2 \times 10^{-4}$ s^{-1} at 55 °C. **1** is the only available catalyst for the smooth transesterification of highly inert simple dialkyl phosphates. From photometric titrations and the pH dependence of reactivity, we conclude that a complex [(**L**)Cu$_2$(DMP)(OCH$_3$)]$^{2+}$ is the reactive species. Steric bulk at the −OR substituents of phosphodiester substrates O$_2$P(OR)$_2^-$ drastically reduces the reactivity of **1**. This is explained with −OR leaving group stabilization by Cu coordination, an interaction which is sensitive to steric crowding at the α-C-atom of substituent R. A proposed reaction mechanism related to that of the exonuclease unit of DNA polymerase I is supported by DFT calculations on reaction intermediates. The complex [(**L**)Cu$_3$(μ_3-OH)-(μ-CH$_3$O)$_2$(CH$_3$CN)$_2$](ClO$_4$)$_3$ (**4**) incorporates a [Cu(OH)(OCH$_3$)$_2$(CH$_3$CN)$_2$]$^-$ complex anion, which might be considered as an analogue of the [PO$_2$(OCH$_3$)$_2$(OCD$_3$)]$^{2-}$ transition state (or intermediate) of DMP transesterification catalyzed by **LCu$_2$**.

Introduction

Phosphoryl transfer reactions are ubiquitous in biology and are usually catalyzed by metalloenzymes. Often two-metal ions appear to be essential for catalytic function. An example is the exonuclease subunit (Klenow fragment) of DNA polymerase I from *E. coli*, which eliminates mismatched nucleotides by phosphodiester bond hydrolysis (Scheme 1, R^1 = 3′-deoxyribosyl, R^2 = 5′-deoxyribosyl, R^3 = H). In vitro the enzyme is active with M$_1$, M$_2$ = Mg^{2+}, Zn^{2+}, Co^{2+}, or Mn^{2+}.

The proposed mechanism shown in Scheme 1 is supported by a crystal structure of the enzyme with a dinuclear Zn/Mg active site and a bound deoxydinucleotide.[1] The phosphodiester unit of the dinucleotide interacts with the dimetal site by three coordinative bonds such as shown in Figure 1, left. Metal ligand distances are between 1.9 and 2.2 Å, and the two-metal ions are 3.9 Å apart. The metal ions provide double Lewis-acid activation of the phosphodiester substrate, activate H$_2$O for nucleophilic attack at P (formation of M−OH nucleophile at neutral pH), and stabilize the OR^1-leaving group. This or related mechanisms might be of wide importance in enzymatic phosphoryl transfer and have subsequently been proposed for phosphate monoester cleavage by *E. coli* alkaline phosphatase (Scheme 1, R^1 = alkyl, R^3 = H),[2] involving a transesterification step, for restriction endonucleases,[3] for DNA polymerases[4] (Scheme 1, R^1 = P$_2$O$_6^{3-}$, R^2 = 5′-deoxy-ribosyl, R^3 = 3′-deoxy-ribosyl), and was discussed as a possible mechanism of RNA cleavage by ribozymes.[5]

Scheme 1. Proposed Mechanism of Phosphodiester Hydrolysis by the Exonuclease Subunit (Klenow Fragment) of DNA Polymerase I

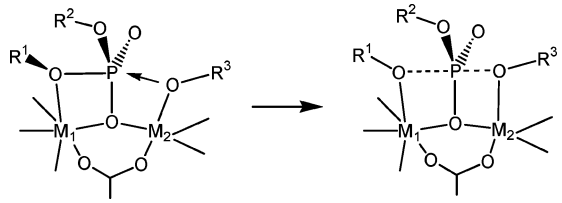

The two-metal mechanism has, however, also been been critically discussed, considering that the presence of two-metal ions in the active site might (at least in some cases) be an artifact

[†] Anorganisch-Chemisches Institut, Universität Heidelberg.
[‡] IWR, Universität Heidelberg.

(1) Beese, L. S.; Steitz, T. A. *EMBO J.* **1991**, *10*, 25−33.
(2) Kim, E. E.; Wyckoff, H. W. *J. Mol. Biol.* **1991**, *218*, 449−464.
(3) Kovall, R. A.; Matthews, B. W. *Curr. Opin. Chem. Biol.* **1999**, *3*, 578−583.
(4) Steitz, T. A. *J. Biol. Chem.* **1999**, *247*, 17395−17398; *Nature* **1998**, *391*, 231−232.
(5) Steitz, T. A.; Steitz, J. A. *Proc. Natl. Acad. Sci. U.S.A.* **1993**, *90*, 6498−6502.

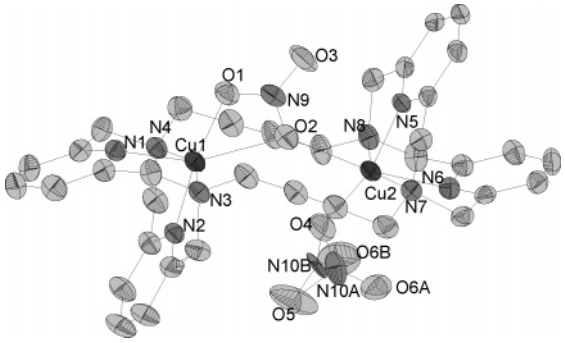

Figure 1. Crystal structure of the $[(\mathbf{L})Cu_2(NO_3)_2]^{2+}$ complex cation of **1**. Hydrogen atoms are omitted for clarity. One of the coordinated nitrate ligands is disordered (N(10a), N(10b)). Selected bond lengths [Å] and angles [deg]: Cu(1)---Cu(2) 4.78, Cu(1)−N(1) 2.128(4), Cu(1)−N(2) 1.944(4), Cu(1)−N(3) 2.169(4), Cu(1)−N(4) 2.191(4), Cu(1)−O(1) 1.954(4), Cu(1)−O(2) 2.500(4), Cu(2)−N(5) 1.946(4), Cu(2)−N(6) 2.155(4), Cu(2)−N(7) 2.228(4), Cu(2)−N(8) 2.209(4), Cu(2)−O(4) 1.907(5), Cu(2)−O(2) 2.524(4); N(1)−Cu(1)−N(2) 86.4(2), N(3)−Cu(1)−N(4) 154.5(2), O(2)−Cu(2)−O(4) 76.4(2), N(5)−Cu(2)−N(6) 83.0(2), N(7)−Cu(2)−N(8) 152.6(2).

of the high concentration of metal ion used to soak the crystal prior to structure analysis, and the use of "nonnatural" metal ions that might have different binding specifities. Biochemical studies have been presented for the exonuclease subunit of DNA polymerase I that support a one-metal mechanism under "natural" conditions;[6] others have shown the necessity of two-metal ions[7] for efficient catalysis.

Many important studies using simple coordination compounds gave insight into various modes for two-metal activation of phosphoryltransfer.[8−10] In most cases, the substrates were reactive phosphate esters, either with good leaving groups (such as nitrophenolate) or with neighboring −OH as a catalytic auxiliary group (as present in RNA), or supercoiled plasmid DNA, which is activated by intrinsic strain. Although simple dialkyl phosphates such as $O_2P(OCH_3)_2^-$ represent more appropriate models for many biological phosphate transfer reactions than activated aryl phosphates, very few examples of the cleavage of such phosphates by synthetic reagents have been reported. The reason is that these substrates are highly inert: stoichiometric hydrolysis has been observed only with strongly Lewis-acidic tri- and tetravalent metal ions at high temperature or low pH.

It is obvious from the model studies that cooperation of two-metal ions can significantly improve catalytic efficiency, in particular by double Lewis-acid activation of the phosphoester substrate by two-metal ions. However, reaction mechanisms related to Scheme 1 are supported by experimental data only in very rare cases. Bruice and co-workers reported very efficient hydrolysis of a dialkyl phosphonate by cooperative action of three La^{3+} ions and suggested an important contribution of the metal ion in leaving group stabilization.[11] Anchoring chinolyl donors that preorganize the metal ions have been incorporated in the substrate, and the reaction is stoichiometric because metal ions are masked by the reaction products. Crystallographically characterized structural model complexes (dicopper(II), dinickel(II)) for the unusual monodentate 1,1-bridging mode of a phosphodiester were reported by Lippard and co-workers.[12]

We have communicated[13] a preliminary study of a diuclear macrocyclic Cu(II) complex **LCu_2**, which promotes the cleavage of dimethyl phosphate by alcohols. **LCu_2** is the only available catalyst for the transesterification of simple dialkyl phosphates. We have suggested that the unique reactivity of this complex is related to a reaction mechanism similar to that proposed for the Klenow fragment (Scheme 1). Therefore, the complex could serve as a low molecular-weight model for the investigation of the two-metal mechanism suggested for many phosphoryl transfer enzymes. Here, we present a more detailed study on the properties and reactivity of this complex.

Experimental Section

Materials and Methods. All reagents unless otherwise indicated were of analytical grade and were used without further purification. Sodium dimethyl phosphate (DMP) and sodium diethyl phosphate were prepared by reported procedures.[14] Lithium methyl *p*-nitrophenyl phosphate was prepared as described.[15]

UV−vis spectra were measured on a Varian Cary 100-Bio UV−visible spectrophotometer equipped with a temperature controller. Electrospray ionization mass spectra were acquired using Waters ESI-Q-TOF Ultima API device (mobile phase, acetonitrile; flow rate, 50 μL/min). HPLC analysis of **L** was performed on a Waters Alliance liquid chromatograph equipped with UV−vis detector. A Macherey-Nagel Nucleosil C18 250 × 4.6 mm column with gradients of CH_3CN/water was used. EPR spectra were recorded on a Bruker ESP 300E spectrometer in methanol glass at 77 K. ^{1}H NMR spectra were acquired using a Bruker AC200 spectrometer (200 MHz).

The $CH_3OH_2^+$ concentration was determined using a Thermo-ORION 420A pH meter equipped with an ORION 7103SC combination (glass/calomel) electrode, calibrated with Acros Organic standard aqueous buffers (pH = 4 and pH = 7). Values of ^{s}pH[16] were obtained

(6) Black, C. B.; Cowan, J. A. *J. Biol. Inorg. Chem.* **1998**, *3*, 292−299.
(7) Curley, J. F.; Joyce, C. M.; Piccirilli, J. A. *J. Am. Chem. Soc*. **1997**, *119*, 12691−12692.
(8) Reviews: (a) Williams, N. H.; Takasaki, B. *J. Chin. Acc. Chem. Res.* **1999**, *32*, 485−493. (b) Blasko, A.; Bruice, T. C. *Acc. Chem. Res.* **1999**, *32*, 475−484. (c) Krämer, R.; Gajda, T. *Perspect. Bioinorg. Chem.* **1999**, *4*, 209−240. (d) Kimura, E. *Curr. Opin. Chem. Biol.* **2000**, *4*, 207−213. (e) Calama, M. C.; Timmermann, P.; Reinhoudt, D. N. *Chem. Soc. Rev*. **2000**, *29*, 75−86.
(9) More recent examples of dicopper(II) systems: (a) Mancin, F.; Rampazzo, E.; Tecilla, P.; Tonellato, U. *Eur. J. Org. Chem.* **2004**, *2*, 281−288. (b) Jancso, A.; Mikkola, S.; Lonnberg, H.; Hegetschweiler, K.; Gajda, T. *Chem.-Eur. J.* **2003**, *9*, 5404−5415. (c) Fry, F. H.; Spiccia, L.; Jensen, P.; Moubaraki, B.; Murray, K. S.; Tiekink, E. R. T. *Inorg. Chem.* **2003**, *42*, 5594−5603. (d) Scarpellini, M.; Neves, A.; Hoerner, R.; Bortoluzzi, A. J.; Szpoganics, B.; Zucco, C.; Silva, R. A. N.; Drago, V.; Mangrich, A. S.; Ortiz, W. A.; Passos, Wagner, A. C.; De Oliveira, M. C. B.; Terenzi, H. *Inorg. Chem.* **2003**, *42*, 8353−8365. (e) Gajda, T.; Duepre, Y.; Toeroek, I.; Harmer, J.; Schweiger, A.; Sander, J.; Kuppert, D.; Hegetschweiler, K. *Inorg. Chem.* **2001**, *40*, 4918−4927. (f) Deal, K. A.; Park, G.; Shao, J.; Chasteen, N. D.; Brechbiel, M. W.; Planalp, R. P. *Inorg. Chem.* **2001**, *40*, 4176−4182.
(10) More recent examples of dizink(II) systems: (a) Yang, M. Y.; Iranzo, O.; Richard, J. P.; Morrow, J. R. *J. Am. Chem. Soc.* **2005**, *127*, 1064−1065. (b) Bauer-Siebenlist, B.; Meyer, F.; Farkas, E.; Vidovic, D.; Cuesta-Seijo, J. A.; Herbst-Irmer, R.; Pritzkow, H. *Inorg. Chem.* **2004**, *43*, 4189−4202. (c) Yashiro, M.; Kaneiwa, H.; Onaka, K.; Komiyama, M. *Dalton Trans*. **2004**, *4*, 605−610. (d) Iranzo, O.; Richard, J. P.; Morrow, J. R. *Inorg. Chem.* **2004**, *43*, 1743−1750. (e) Arca, M.; Bencini, A.; Berni, E.; Caltagirone, C.; Devillanova, F. A.; Isaia, F.; Garau, A.; Giorgi, C.; Lippolis, V.; Perra, A.; Tei, L.; Valtancoli, B. *Inorg. Chem.* **2003**, *42*, 6929−6939.
(11) (a) Tsubouchi, A.; Bruice, T. C. *J. Am. Chem. Soc.* **1994**, *116*, 11614−11615. (b) Tsubouchi, A.; Bruice, T. C. *J. Am. Chem. Soc.* **1995**, *117*, 7399−7411.
(12) (a) He, C.; Lippard, S. J. *J. Am. Chem. Soc.* **2000**, *122*, 184−185. (b) He, C.; Gomez, V.; Spingler, B.; Lippard, S. J. *Inorg. Chem.* **2000**, *39*, 4188−4189.
(13) Kuehn, U.; Warzeska, S.; Kraemer, R. *J. Am. Chem. Soc.* **2001**, *123*, 8125−8126.
(14) McIvor, R. A.; McCarty, G. D.; Grant, G. A. *Can. J. Chem.* **1956**, *34*, 1819−1832.
(15) Kirby, A. J.; Younas, M. *J. Chem. Soc. B* **1970**, 1165−1172.
(16) *Compendium of Analytical Nomenclature. Definitive Rules 1997*, 3rd ed.; Blackwell: Oxford, U.K., 1998.

by adding a correction constant of 2.24 to the experimental pH meter reading, as reported by Bosch and co-workers.[17b]

Syntheses. L. 0.25 g (0.67 mmol) of 3,8,16,21,27,28-hexaazatricyclo[21.3.1.110,14]-octacosa-1(27),10,12,14(28),23,25-hexaene-5,18-diine,[18] 0.60 g (1.34 mmol) of 2,6-pyridinedimethyl ditosylate, and 5.00 g (47.2 mmol) of Na_2CO_3 were suspended in 100 mL of acetonitrile and supersonicized for 2 h. After the mixture was stirred for 4 days at room temperature, the solid was filtered off. The filtrate was reduced to 50 mL. 20 mL of water was added dropwise under continuous stirring. The white precipitate was filtered off, washed with water, acetonitrile, and diethyl ether, and dried in vacum. Yield: 191 mg (49%). ESI-MS: *m*/*z* 581 [L + H^+]. ^{1}H NMR ($CDCl_3$): δ [ppm] = 7.11 (t, 4H, 3*J* = 7.6 Hz), 6.80 (d, 8H, 3*J* = 7.6 Hz), 4.69 (d, 8H, 2*J* = 12.3 Hz), 3.97 (d, 8H, 2*J* = 12.3 Hz), 3.93 (s, 8H). UV−vis: λ_{max} (ϵ M^{-1} cm^{-1}); chloroform, 260 nm (9.56×10^3). IR (KBr 4000−400 cm^{-1}): $\tilde{\nu}$ (cm^{-1}) 3389 (s), 3059 (m), 2916 (m), 2841 (m), 1632 (m), 1591 (s), 1454 (s), 1373 (m), 1318 (m), 1277 (m), 1244 (m), 1205 (m), 1155 (m), 1107 (s), 1067 (m), 987 (m), 958 (m), 869 (m), 817 (s), 758 (m), 668 (m), 587 (m), 503 (m), 445 (m). Microanalysis calculated for **L**·$2H_2O$ (%): C, 70.11; H, 6.54; N, 18.16. Found (%): C, 70.37; H, 6.21; N, 17.87.

[(L)$Cu_2(NO_3)_2$]$(NO_3)_2$·$2CH_3OH$ (1). A methanolic solution of 16 mg (66 μmol) of copper(II) nitrate trihydrate was added to a suspension of 20 mg (33 μmol) of **L**·$2H_2O$ in 2 mL of methanol with stirring. A clear green solution was obtained. Layering with diethyl ether yielded a green powder and some green crystals of **1**. The crystals were mechanically separated from the powder. Yield: 5−20%. UV−vis: λ_{max} (ϵ M^{-1} cm^{-1}); methanol/acetonitrile (1:1), 778 nm (160), 260 nm (1.46×10^4). IR (KBr 4000−400 cm^{-1}): $\tilde{\nu}$ (cm^{-1}) 3336 (m), 2921 (m), 2852 (m), 1745 (w), 1729 (w), 1664 (m), 1600 (m), 1447 (m), 1383 (s), 1351 (m), 1256 (m), 1164 (m), 1082 (m), 1033 (m), 949 (m), 866 (w), 801 (m). Microanalysis calculated for [(*L*)$Cu_2(NO_3)_2$]$(NO_3)_2$·$2CH_3OH$ (%): C, 44.75; H, 4.35; N, 16.48. Found (%): C, 44.46; H, 4.00; N, 16.03.

[(L)Cu_2(μ-CO_3)(CH_3OH)]$(BF_4)_2$·$2CH_3OH$ (2). A methanolic solution of 23 mg (67 μmol) of copper(II) tetrafluoroborate hexahydrate was added to 20 mg (33 μmol) of **L**·$2H_2O$ suspended in 2 mL of methanol. The light blue suspension turned into a green solution when 15 mg of solid $NaHCO_3$ was added with stirring. After 30 min, excess $NaHCO_3$ was removed by centrifugation and the solution was layered with diethyl ether. X-ray quality green crystals of [(**L**)Cu_2(μ-CO_3)(CH_3OH)]$(BF_4)_2$·$2CH_3OH$ were obtained after 1 day. Yield: 30%. UV−vis: λ_{max} (ϵ M^{-1} cm^{-1}); methanol, 747 nm (94), 336 nm (4.4×10^3), 261 nm (1.71×10^4). IR (KBr 4000−400 cm^{-1}): $\tilde{\nu}$ (cm^{-1}) 3442 (m), 2925 (m), 2838 (m), 1604 (m), 1581 (m), 1471 (m), 1400 (m), 1310 (m), 1209 (m), 1165 (m), 1082 (s), 1059 (s), 959 (m), 908 (w), 881 (m), 827 (w), 789 (m), 760 (m), 688 (w), 519 (w), 457 (w). Microanalysis calculated for [(**L**)$Cu_2(CO_3)(CH_3OH)](BF_4)_2$·$2CH_3OH$ (%): C, 46.30; H, 4.66; N, 10.80. Found (%): C, 46.81; H, 4.83; N, 11.18.

[(L)Cu_2(1,3-μ-DMP)(NO_3)]$(NO_3)_2$·CH_3OH·H_2O (3). To 30 mg (49 μmol) of **L**·$2H_2O$ suspended in 4 mL of methanol were added 24 mg (100 μmol) of $Cu(NO_3)_2$·$3H_2O$ and 7.7 mg (52 μmol) of NaDMP. A green solution is obtained under stirring. Layering with diethyl ether yields some blue-green crystals of [(**L**)Cu_2(μ-DMP)$(NO_3)_2$]$(NO_3)_2$. The yield was too small for full characterization, and crystallization was not reproducible.

[(L)Cu_3(μ_3-OH)(μ-CH_3O)$_2$(CH_3CN)$_2$]$(ClO_4)_3$·CH_3CN (4). To 6.0 mg (10 μmol) of **L** suspended in 1 mL of acetonitrile was added 11 mg (30 μmol) of $Cu(ClO_4)_2$·$6H_2O$ in 1 mL of methanol, and a bluish-green solution was obtained. After layering with diethyl ether, blue-green crystals of [(**L**)Cu_3(μ_3-OH)(μ-CH_3O)$_2$(CH_3CN)$_2$]$(ClO_4)_3$ were obtained. Again, the yield was too small for full characterization, and crystallization was difficult to reproduce.

In Situ Preparation of Complexes LM_2 in Solution. By reaction of **L** with 2 equiv of $Cu(NO_3)_2$·$3H_2O$ or anhydrous $CuBr_2$ in CD_3OD at 50 °C, green solutions are obtained. These solutions most likely contain a mixture of complex species but are both active in DMP transesterification, although they are about 5 times less efficient than isolated crystals of **1**. On the basis of this observation, we performed a qualitative test of transesterification activity by preparing a 2 mM solution in CD_3OD of **L**+1 or 2 equiv of anhydrous $ZnBr_2$. The solutions were used for catalytic assays as described for **1**/DMP with reaction control by ^{1}H NMR spectroscopy. None of the in situ prepared complexes **L**+$2Zn^{2+}$ or **L**+Cu^{2+}+Zn^{2+} shows any transesterification activity after 1 week at 55 °C.

Catalytic Transesterification of Dialkyl Phosphates in CD_3OD. In a typical kinetic assay, 7.4 mg (50 μmol) of sodium dimethyl phosphate was added to 1 mL of a 2 mM stock solution of **1** in CD_3OD, and the solution was transferred to an NMR tube. The sample was kept at either 25 or 55 °C, and ^{1}H NMR spectra were recorded in appropriate time intervals. Conversion of $O_2P(OCH_3)_2^-$ to $O_2P(OCH_3)$-$(OCD_3)^-$ was followed by integration of the signals of released methanol and residual methyl ester. The same procedure was applied to the transesterification of other phosphodiesters.

pH Determination in CH_3OH. The pH values of methanolic solutions were obtained with an ORION 7103SC combination (glass/calomel) electrode at 25 °C. pH meter reading was stable after about 30 s equilibration time. The recommended[17b] correction value 2.24 was added to the pH meter reading to obtain ^{s}pH.

Spectrophotometric Titration. A solution of **1** (100 μM) was prepared in methanol. Aliquots of stock solutions containing NaDMP or CO_2-free $NaOCH_3$ (20 mM in methanol) were added with stirring. Immediately after addition, a UV spectrum of the solution was taken at 25 °C. A volume correction of absorbance was not performed because the total volume of added NaDMP or $NaOCH_3$ does not exceed 2% of the reaction solution.

Structure Determinations. Details of the crystal data and refinement are given in Table 1. Intensities were collected using a Bruker AXS CCD Smart 1000 (for **3** and **4**) or SIEMENS P3 (for **1** and **2**) diffractometer, both with graphite-monochromated Mo Kα radiation (λ = 0.71073 Å). Corrections for Lorentz and polarization effects were applied. Absorption corrections were performed on the basis of multiple scans of equivalent reflections using the SADABS routine. The structures were solved by direct methods and refined by full-matrix least-squares (SHELXTL-PLUS for **1** and **2**; SHELXTL NT V.5.1 for **3** and **4**) anisotropically for all non-hydrogen atoms. Hydrogen atoms were located in difference Fourier maps and refined isotropically. Crystal data details for **1**, **2**, **3**, and **4** are given in Table 1.

DFT Calculation. The calculations were performed using the program package TURBOMOLE 5.7.[19] We applied the B3LYP density functional together with the LANL2DZ basis set with an effective core potential for the copper atoms and the SVP all electron basis set for all of the other atoms.

The computations started from the crystal structure of the [(**L**)$Cu_2(DMP)(NO_3)]^{2+}$ replacing the nitrate ion with a methanolate ion. This starting structure was fully optimized in a vacuum. Further vacuum minimum energy structures were obtained from starting structures derived by modification of the latter (terminally coordinated methanolate, bridging phosphate etc.). Minimizations were carried out stepwise: First, the methanolate−oxygen−copper distance and the O−Cu−O(phosphate) angle were fixed while all other degrees of freedom were optimized. Subsequently, the fixed internal coordinates

(17) (a) Neverov, A. A.; Brown, R. S. *Inorg. Chem.* **2001**, *40*, 3588−3595. (b) Bosch, E.; Rived, F.; Roses, M.; Sales, J. *J. Chem. Soc., Perkin Trans. 2* **1999**, 1953−1958.
(18) Warzeska, S.; Kraemer, R. *Chem. Ber*. **1995**, *128*, 115−119.
(19) Electronic Structure Calculations on Workstation Computers: The Program System TURBOMOLE. Ahlrichs, R.; Bar, M.; Haser, M.; Horn, H.; Kolmel, C. *Chem. Phys. Lett.* **1989**, *162*, 165.

Table 1. Crystal Data and Structure Refinement for **1**, **2**, **3**, and **4**

	1	2	3	4
empirical formula	$C_{38}H_{44}Cu_2N_{12}O_{14}$	$C_{40}H_{48}B_2Cu_2F_8N_8O_6$	$C_{39}H_{48}Cu_2N_{11}O_{15}P$	$C_{44}H_{52}Cl_3Cu_3N_{11}O_{15}$
formula weight	1019.93	1037.56	1068.93	1271.94
crystal size (mm^3)	0.30 × 0.32 × 0.35	0.35 × 0.38 × 0.30	0.22 × 0.08 × 0.03	0.24 × 0.18 × 0.06
crystal system	monoclinic	monoclinic	orthorhombic	orthorhombic
space group	$P2_1/c$	$P2_1/c$	*Pbca*	*Pnma*
a (Å)	18.151(4)	10.323(5)	14.5986(16)	18.8716(10)
b (Å)	14.728(3)	13.178(7	20.862(2)	18.4126(9)
c (Å)	16.064(3)	31.611(17	28.726(3)	14.8895(8)
α (deg)	90	90	90	90
β (deg)	96.93(3)	94.41	90	90
γ (deg)	90	90	90	90
volume	4263(2)	4287.5(38)	8748.7(16)	5173.7(5)
Z	4	4	8	4
temperature (K)	170	170	100(2)	173(2)
R indices (all data)	R1 = 0.1313, wR2 = 0.1625	R1 = 0.0658, wR2 = 0.1499	R1 = 0.1485, wR2 = 0,1239	R1 = 0.0637, wR2 = 0.1141
GOF on F^2	1.015	0.986	0.821	1.005

Scheme 2. Synthesis of **L** and HPLC−MS Analysis of Reaction Product[a]

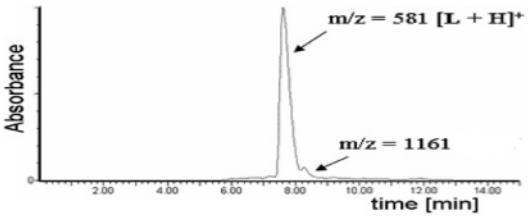

[a] The peak at *m*/*z* = 1161 is attributed to trace of a covalent "dimer" formed by reaction of two molecules of the hexaazamacrocycle with four molecules of the ditosylate.

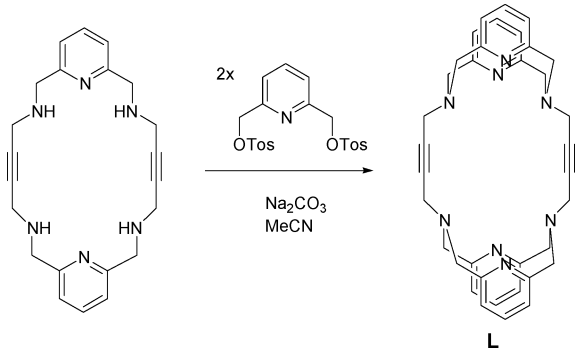

were relaxed and the structures were fully optimized to a convergence criterion of 10^{-6} au and 10^{-4} au/bohr for energy and gradient, respectively.

Solvent effects were treated implicitly, making use of the conductor like screening model (COSMO) as implemented in TURBOMOLE. This approach is a dielectric continuum solvation model in which the mutual polarization of the solute and the solvent is represented by screening charges on the surface of the solute cavity. These charges are derived under the simplified boundary condition that the electrostatic potential vanishes for a conductor and then are scaled to account for the finite dielectric constant of a real solvent (here methanol). All minimum energy structures, except **B**, obtained from vacuum calculations were reoptimized in implicit methanol to 10^{-6} au and 10^{-3} au/bohr for energy and gradient, respectively. For **B**, no stable vacuum minimum could be trapped. Thus, optimization of this structure in implicit solvent started from the initial starting structure for the vacuum calculations. Analytical second derivatives with subsequent normal-mode analyses were carried out on the optimized structures to verify the minima.

Results and Discussion

Ligand Synthesis. The synthesis of dinucleating octaaza macrocycle **L** from a hexaazamacrocyclic precursor was communicated before but has not yet been described in detail.[18] **L** is obtained by N-alkylation with 2,6-pyridinedimethyl ditosylate (2 equiv) in acetonitrile in the presence of Na_2CO_3 with up to 49% yield (Scheme 2). HPLC−MS analysis of the product indicates formation of trace amounts (<5%) of "oligomeric" byproducts, which could not be removed by crystallization or column chromatography.

Metal Complex Synthesis. The dinuclear Cu(II) complex $[(\mathbf{L})Cu_2(NO_3)_2](NO_3)_2 \cdot 2CH_3OH$ (**1**) is obtained by reaction of **L** with 2 equiv of $Cu(NO_3)_2$ trihydrate in methanol. This complex, which is used as a phosphoryltransfer catalyst,could be isolated in pure, crystalline form but only in low yield. We attribute this low yield to a surprising kinetic stability of the Cu(II) complexes of **L**. Instead of smooth formation of the thermodynamically most stable product, complex formation might be under kinetic control. ESI spectra of a mixture of **L** and 2 equiv of $Cu(NO_3)_2$ in methanol display signals of $[(\mathbf{L})Cu]^{2+}$, $[(\mathbf{L})Cu(OH^-)(H_2O)]^+$, and $[(\mathbf{L})Cu_2(NO_3^-)_2(OH^-)]^+$, while isolated crystals of **1** in methanol show only signals of the dinuclear species. The yield of **1** could not be improved by variation of reaction conditions (e.g., synthesis at prolonged reaction time at 50 °C).

A carbonate complex $[(\mathbf{L})Cu_2(\mu\text{-}CO_3)(CH_3OH)](BF_4)_2$ **2** was prepared from **L**, $Cu(BF_4)_2 \cdot 6H_2O$, and $NaHCO_3$ in methanol. Many attempts to isolate phosphate ester complexes of $\mathbf{LCu_2}$ were unsuccessful, except for the case of dimethyl phosphate complex **3**, which could, however, not be fully characterized because it was obtained in very low yield and its crystallization was not reproducible. The trinuclear complex $[(\mathbf{L})Cu_3(\mu_3\text{-}OH)(\mu\text{-}CH_3O)_2(CH_3CN)_2](ClO_4)_3$ **4** is formed by reaction of **L** and 3 equiv of $Cu(ClO_4)_2 \cdot 6H_2O$ and is considered as a complex of $\mathbf{LCu_2}$ with a transition state analogue of dimethyl phosphate transesterification (see below). Again, the synthesis of this complex was difficult to reproduce.

We have prepared complexes of **L** with Zn^{2+} ions in situ by mixing **L** and 2 equiv of the metal salt in MeOH or CD_3OD at 55 °C. We could not isolate the complexes, but UV spectrophotometry indicates that, as in the case of Cu^{2+}, a 1:1 complex forms rapidly and additional metal ion is incorporated only after prolonged heating of the solution. None of the complexes $\mathbf{L}+2Zn^{2+}$ and $\mathbf{L}+Cu^{2+}+Zn^{2+}$ prepared in CD_3OD solution had any activity in DMP transesterification at 55 °C.

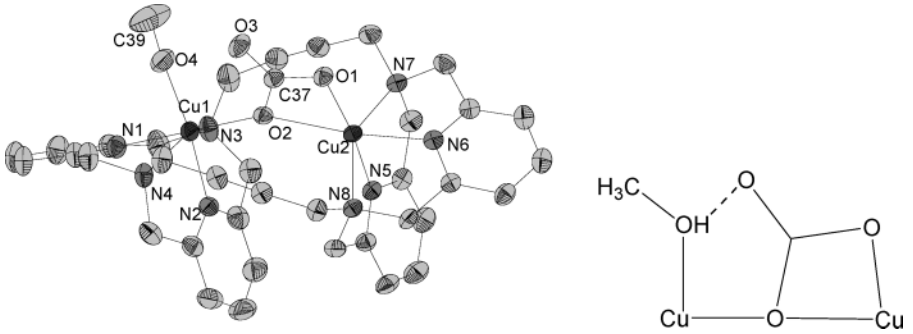

Figure 2. Left: molecular structure of the $[(\mathbf{L})Cu_2(\mu\text{-}CO_3)(CH_3OH)]^{2+}$ complex cation of **2**. Hydrogen atoms are omitted for clarity. Right: $Cu_2(\mu\text{-}CO_3)(CH_3OH)$ unit. Selected bond lengths [Å] and angles [deg]: Cu(1)---Cu(2) 4.18, Cu(1)−N(1) 2.030(3), Cu(1)−N(2) 1.982(3), Cu(1)−N(3) 2.391(3), Cu(1)−N(4) 2.329(3), Cu(1)−O(2) 2.025(2), Cu(1)−O(4) 1.975(3), Cu(2)−N(5) 1.932(3), Cu(2)−N(6) 2.115(3), Cu(2)−N(7) 2.291(3), Cu(2)−N(8) 2.381(3), Cu(2)−O(1) 1.897(2), Cu(2)−O(2) 2.284(2); N(1)−Cu(1)−N(2) 87.38(11), N(3)−Cu(1)−N(4) 145.87(10), O(2)−Cu(1)−O(4) 91.47(10), Cu(1)−O(2)−Cu(2) 152.29(10), N(5)−Cu(2)−N(6) 84.47(10), N(7)−Cu(2)−N(8) 149.05(9), O(1)−Cu(2)−O(2) 62.54(8).

Metal Complex Structures. It is evident from previous structural studies[20] on the dicopper(II) complexes of **L** that the coordination geometry of the Cu ions depends on the presence or absence of a bridging coligand. In the presence of bridging ligands, the coordination of Cu ions is elongated octahedral with four short in-plane bonds and two elongated apical bonds to the sp^3 nitrogens of the tetradentate diazapyridinophane-type subunit. Such a coordination is comparable to that reported for mononuclear Cu(II) complexes of 2,11-diaza[3.3](2,6)pyridinophanes.[21]

In the absence of a bridging coligand, however, an octahedral coordination by addition of two monodentate coligands at each Cu in **LCu$_2$** is sterically hindered. In such complexes, the copper ions display five coordination with strong rhombic distortion of the basal plane.[20] These complexes have a very high tendency to incorporate bridging anions.

The structure of the $[(\mathbf{L})Cu_2(NO_3)_2]^{2+}$ cation of **1** is shown in Figure 1. The Cu(II) ions are four-coordinated by the pyridinophane subunits of **L**. Additionally, each Cu forms a short bond to a nitrate oxygen atom, Cu(1)−O(1) and Cu(2)−O(4), respectively. A bridging nitrate oxygen O(2) may be considered as a sixth ligand at Cu, but the interaction is rather weak (Cu−O ≈ 2.5 Å). The N3−O basal plane displays a significant rhombic distortion, similar to the five-coordinate **LCu$_2$** complexes.[20] The solution structure of **1** in MeOH glass appears to be similar because an EPR signal $g_\perp = 2.13$ with strong rhombic splitting is observed.

In the carbonate complex **2** (Figure 2), the Cu−O bonds to the bridging carbonate O(2)-atom are much shorter as compared to **1**, and the Cu ion coordination is best described as distorted octahedral with elongation along the N(sp^3)−Cu−N(sp^3) axes. This structure is important with respect to the proposed Klenow fragment mechanism (Scheme 1) because it confirms the unusual 1,1-μ coordination mode of an oxoanion together with the coordination of a CH_3OH solvent molecule (which is a potential nucleophile) in the model complex. The Cu−Cu distance of 4.18 Å in **2** is somewhat larger than the Mg−Zn distance of 3.9 Å in the dinucleotide complex of the Klenow fragment.

Structural data of poor quality were obtained for the dimethyl phosphate complex $[(\mathbf{L})Cu_2(1,3\text{-}\mu\text{-DMP})(NO_3)](NO_3)_2$ (**3**) (Figure 3), which crystallized from a methanolic 1:1 mixture of **1** and NaDMP. While dimethyl phosphate coordinates by O(1) and O(2) in a 1,3-bridging fashion, the nitrate ligand forms only one short Cu(1)−O(5) bond (distance of O(5) to Cu(2) is 3.007 Å and thus nonbonding). This results in a mixed coordination of the Cu ions, elongated octahedral Cu(1) and five-coordinate Cu(2).

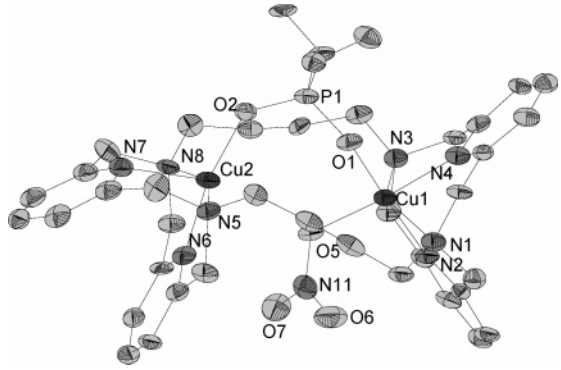

Figure 3. Crystal structure of the $[(\mathbf{L})Cu_2(1,3\text{-}\mu\text{-DMP})(NO_3)]^{2+}$ complex cation of **3**. Hydrogen atoms are omitted for clarity. Selected bond lengths [Å] and angles [deg]: Cu(1)−O(1) 1.922(4), Cu(1)−N(2) 1.978(5), Cu(1)−O(5) 1.996(4), Cu(1)−N(4) 2.008(5), Cu(1)−N(1) 2.352(5), Cu(1)−N(3) 2.435(5), Cu(2)−O(2) 1.883(4), Cu(2)−N(6) 1.924(5), Cu(2)−N(7) 2.169(5), Cu(2)−N(5) 2.218(5), Cu(2)−N(8) 2.227(5); O(1)−Cu(1)−N(2) 174.5(2), O(1)−Cu(1)−O(5) 90.31(17), N(2)−Cu(1)−O(5) 93.40(19), O(1)−Cu(1)−N(4) 89.47(19), N(2)−Cu(1)−N(4) 87.4(2), O(5)−Cu(1)−N(4) 171.9(2), N(1)−Cu(1)−N(3) 143.75(18), O(2)−Cu(2)−N(6) 168.86(19), O(2)−Cu(2)−N(7) 107.17(18), N(6)−Cu(2)−N(7) 83.8(2), N(5)−Cu(2)−N(8) 153.07(19).

The trinuclear complex **4** (Figure 4) can be described as **LCu$_2$** incorporating an anionic $[Cu(\mu\text{-}OH)(\mu\text{-}OCH_3)_2(NCCH_3)_2]^-$ complex fragment. Macrocycle-bound Cu(1) and Cu(2) have an elongated octahedral coordination, and the coordination of Cu(3) is between square planar and trigonal bipyramidal. This structure is relevant to the mechanistic discussion (see below) because $[Cu(\mu\text{-}OH)(\mu\text{-}OCH_3)_2(NCCH_3)_2]^-$ might be considered as a transition state analogue of dimethyl phosphate transesterification by CD_3OD, a reaction which is efficiently catalyzed by **LCu$_2$**. Moreover, there are analogies between complex **4** and the proposed transition state stabilization in phosphodiester hydrolysis by the Klenow fragment of DNA polymerase I and phosphate monoester transesterification by *E. coli* alkaline phosphatase.

Bonding parameters within the T-shaped Cu(2)$(OCH_3)_2$O(1)H fragment are related to those of the P$(OCH_3)_2$O moiety (P−OCH_3 1.87 Å, P−O 1.52 Å) in P$(OCH_3)_3O_2^{2-}$, the ab initio

(20) Warzeska, S.; Kraemer, R. *Chem. Commun*. **1996**, 499−500.
(21) (a) Fronczek, F. R.; Mamo, A.; Pappalardo, S. *Inorg. Chem.* **1989**, *28*, 1419−22. (b) Che, C. M.; Li, Z. Y.; Wong, K. Y.; Poon, C. K.; Mak, T. C. W.; Peng, S. M. *Polyhedron* **1994**, *13*, 771−6. (c) Krueger, H. J. *Chem. Ber*. **1995**, *128*, 531−9.

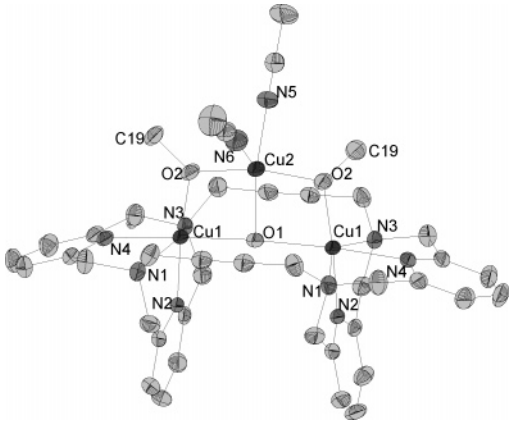

Figure 4. Crystal structure of the $[\mathbf{L}Cu_3(\mu\text{-}OH)(\mu\text{-}CH_3O)_2\ (CH_3CN)_2]^{3+}$ cation of **4**. A crystallographic mirror plane passes through O(1), Cu(2), N(5), and N(6). Hydrogen atoms are omitted for clarity. Selected bond lengths [Å] and angles[deg]: Cu(1)---Cu(1) 4.328(5), Cu(1)---Cu(2) 3.0021(6), Cu(1)−O(1) 2.1718(5), Cu(1)−O(2) 1.872(2), Cu(1)−N(1) 2.393(3), Cu(1)−N(2) 1.952(3), Cu(1)−N(3) 2.337(3), Cu(1)−N(4) 2.147(3), Cu(2)−O(1) 1.984(3), Cu(2)−O(2) 1.902(2), Cu(2)−N(5) 2.017(4), Cu(2)−N(6) 2.296(5); Cu(1)−O(1)−Cu(1) 170.20(2), O(1)−Cu(1)−O(2) 78.91(1), O(2)−Cu(1)−N(2) 174.52(1), O(2)−Cu(1)−N(4) 103.49(1), N(1)−Cu(1)−N(3), 147.70(1), N(2)−Cu(1)−N(4) 81.62(1), Cu(2)−O(1)−Cu(1) 92.40(9), Cu(1)−O(2)−Cu(2) 105.40(1), O(2)−Cu(2)−O(2) 165.85(1), O(2)−Cu(2)−O(1) 83.17(7), O(2)−Cu(2)−N(5) 94.97(8), O(2)−Cu(2)−N(6) 95.03(9), N(5)−Cu(2)−N(6) 89.90(2), O(1)−Cu(2)−N(5) 149.89(2), O(1)−Cu(2)−N(6) 120.21(2), C(19)−O(2)−Cu(1) 126.5(2), C(19)−O(2)−Cu(2) 127.2(2).

Scheme 3. $[Cu(OH)(OMe)_2(CH_3CN)_2]^-$ Complex Anion and Ab Initio Calculated Structure of $[(CH_3O)_3PO_2]^{2-}$, the Energy-Rich Intermediate of Dimethyl Phosphate Methanolysis[22]

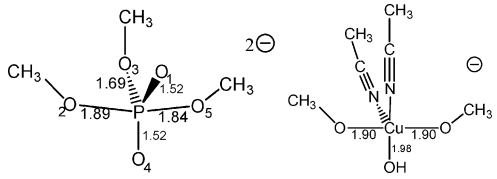

calculated structure of the energy-rich intermediate of dimethyl phosphate methanolysis[22] (Scheme 3).

Solution Chemistry of Cu(II) Complexes of L. Complex formation in methanol/chloroform (the latter was added to improve solubility of **L**) was followed by spectrophotometric titration of **L** with a solution of copper(II) nitrate. A 1:1 **L**−Cu(II) complex is formed smoothly and rapidly. EPR spectra of frozen solution are well resolved and indicate formation of a single species with $g_{||} = 2.29$ and $A_{||} = 154$ G, typical for in-plane N_2O_2-coordination of Cu(II).[23] Therefore, we assume an elongated octahedral coordination by one diazapyridinophane subunit and two solvent (or nitrate) coligands, with in-plane coordination by the latter O-donors and two pyridine N atoms.

Incorporation of a second Cu(II) ion is more difficult to achieve and requires prolonged heating to 50 °C. Distinct spectral changes are observed but are no longer indicative of a smooth conversion.

To investigate the interaction of **1** with dimethyl phosphate in solution, we have performed a UV−vis titration of the complex with NaDMP in methanol. Interaction of $\mathbf{LCu_2}$ with oxoanions is generally followed on the basis of a broad absorbance in the range 300−350 nm (ϵ in the order of 4000 $M^{-1}\ cm^{-1}$), which we interpret as an oxygen-to-copper(II) charge-transfer band. In case of **1**, the band is very broad and appears as a shoulder centered at about 325 nm. On addition of up to ∼1 equiv of DMP to **1**, the shoulder decreases continuously (Figure 5, right), suggesting the formation of a 1:1 $\mathbf{LCu_2}$−DMP complex. Addition of more DMP smoothly generates a new species with an absorbance maximum at 310 nm ($\epsilon_{310} = 4200\ M^{-1}\ cm^{-1}$), but complete conversion (i.e., no further increase of 310 nm absorbance) requires large excess (>20 equiv) of DMP. Because the same changes of absorbance with isosbestic points are observed, when the 1:1 $\mathbf{LCu_2}$−DMP solution is titrated with 0−1 equiv of $NaOCH_3$ (Figure 5), we conclude that a methanolate complex $[(\mathbf{L})Cu_2(DMP)(OCH_3)]^{2+}$ is formed in both cases, by addition of either 1 equiv of OCH_3^- or a large excess of DMP, which is a weak base and deprotonates a Cu-coordinated MeOH solvent molecule. In Figure 5, left, spectra are selected that correspond to the addition of 0 to ∼0.6 equiv of $NaOCH_3$ to the **1**/DMP 1:1 mixture. Titration curves obtained on subsequent $NaOCH_3$ addition no longer pass the isosbestic points, and absorbance no longer increases linearly (Figure 5). Frozen methanolic solutions containing **1** and excess NaDMP show poorly resolved, complicated EPR spectra.

A titration of **1** with $NaOCH_3$ in the absence of DMP reveals only minor spectral changes from 0 to 1 equiv of base, and the spectrum of proposed product $(\mathbf{L})Cu_2(OCH_3)$ is different from that of $(\mathbf{L})Cu_2(OCH_3)$(DMP). $(\mathbf{L})Cu_2(OCH_3)$ converts smoothly to $(\mathbf{L})Cu_2(OCH_3)_2$ at 1−2 equiv of $NaOCH_3$ (Figure 6), with a

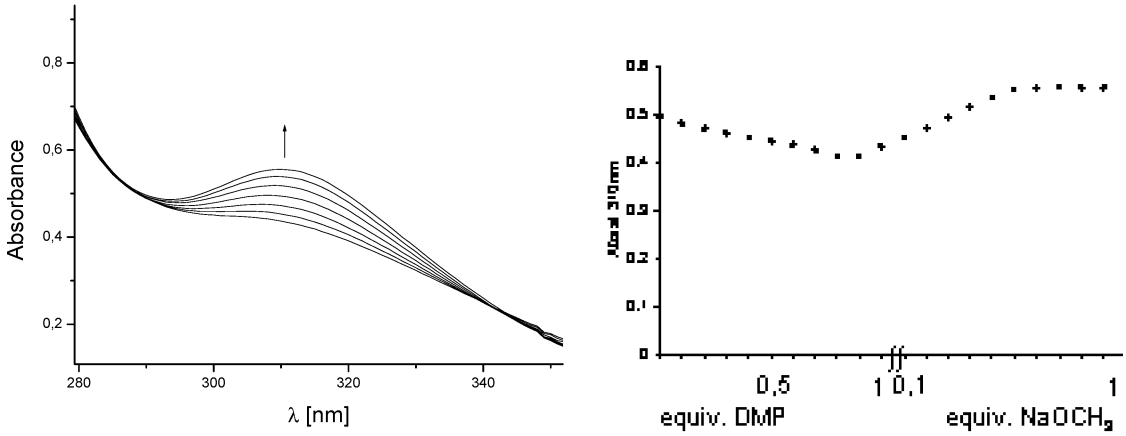

Figure 5. Left: spectrophotometric titration of a methanol solution of **1**/DMP (0.1 mM each) with $NaOCH_3$ (0−0.6 equiv) in 0.1 equiv steps. Right: absorbance diagram at 310 nm of a methanolic solution of **1** (0.1 mM) on addition of 0−1 equiv of DMP, and on subsequent addition of 0−1 equiv of $NaOCH_3$ (in 0.1 equiv steps).

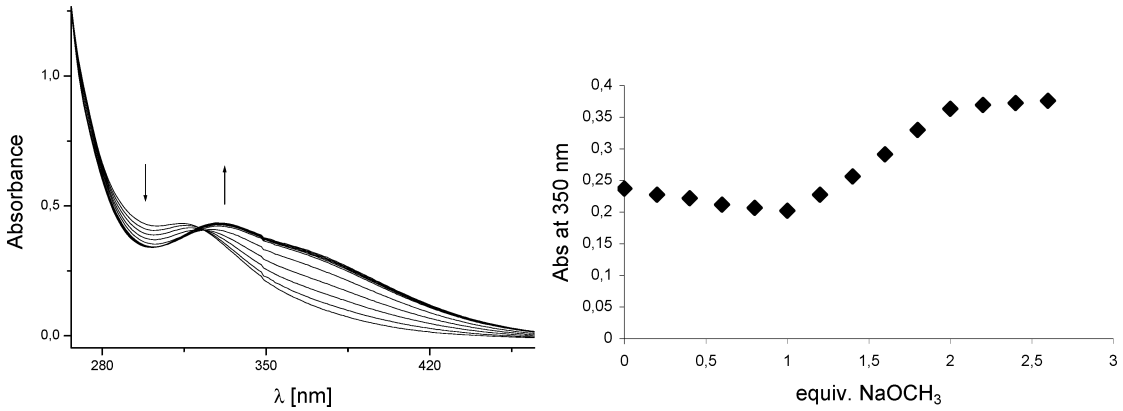

Figure 6. Left: spectrophotometric titration of **1** (0.1 mM) in methanol with $NaOCH_3$ (in 0.2 equiv steps; only the curves for 1−2.5 equiv of $NaOCH_3$ are shown). Right: absorbance diagram at 350 nm for addition of 0−2.5 equiv of $NaOCH_3$ to **1** (0.1 mM).

Scheme 4. Suggested Protonation Equilibria of $\mathbf{LCu_2}$ in Methanolic Solution in the Presence of DMP

$$LCu_2(DMP) \rightleftharpoons LCu_2(DMP)(OCH_3) + H^+ \qquad pK_a = 8.8$$

$$LCu_2(DMP)(OCH_3) \rightleftharpoons LCu_2(OCH_3)_2 + H^+ + DMP \qquad pK_a \approx 12$$

characteristic maximum of the bis(methanolate)complex at 335 nm ($\epsilon_{335} = 4200\ cm^{-1}$). No significant spectral changes are observed on addition of >2 equiv of $NaOCH_3$. Also, the spectrum at 2.2 equiv of $NaOCH_3$ does not change significantly on addition of 25 equiv of NaDMP, indicating that DMP does not strongly compete with the second OCH_3^- for $\mathbf{LCu_2}$ binding.

For the bright green carbonate complex **2**, only a very broad shoulder located at about 335 nm is observed, with significant absorbance at >400 nm, similar to the case of $(\mathbf{L})Cu_2(OCH_3)_2$.

In addition to the spectrophotometric studies, we have performed pH measurements in the methanolic solutions, following a more recently recommended method[17b] using a standard glass electrode calibrated with aqueous buffers and a correction value of +2.24 added to the pH meter reading. We had some problems with the reproducibility of these measurements, but data quality was sufficient for the determination of approximate pK_a values for some of the solution species involved by measuring their half neutralization. A pK_a = 4.9 (±0.2) of HDMP at 1 mM concentration in methanol (no salts added) was determined by titration of NaDMP with the strong acid *p*-toluenesulfonic acid. As expected, this value is somewhat higher than the one reported (3.95) for phosphoric acid diphenyl ester.[17a] pK_a = 6.0 (±0.2) of $\mathbf{LCu_2}(CH_3OH)$ was derived from the pH value at half neutralization of **1**. From the pH titration of $\mathbf{LCu_2}$DMP (1 mM), formed in situ from **1** and NaDMP, with $NaOCH_3$ (Supporting Information), pK_a values of 8.5 (±0.3) and ∼12 (corresponding to the pH on addition of 0.5 and 1.5 equiv of $NaOCH_3$) were derived for the equlibria $\mathbf{LCu_2}$(DMP)/$\mathbf{LCu_2}$(DMP)(OCH_3) + H^+ and $\mathbf{LCu_2}$(DMP)(OCH_3)/$\mathbf{LCu_2}$-$(OCH_3)_2$ + H^+ (Supporting Information).

Conversion of $\mathbf{LCu_2}(OCH_3)$ or $\mathbf{LCu_2}$(DMP)(OCH_3) to $\mathbf{LCu_2}$-$(OCH_3)_2$ requires strongly basic conditions, and the pK_a value could not be determined accurately. A summary of the suggested acid−base equilibria in the presence of DMP is given in Scheme 4.

A calculated pH-dependent distribution of the three complex species of Scheme 4 supports a smooth conversion of $\mathbf{LCu_2}$(DMP) into $\mathbf{LCu_2}$(DMP)(OCH_3) on half neutralization to pH 8.5, while formation of $\mathbf{LCu_2}(OCH_3)_2$ becomes significant at pH > 11.

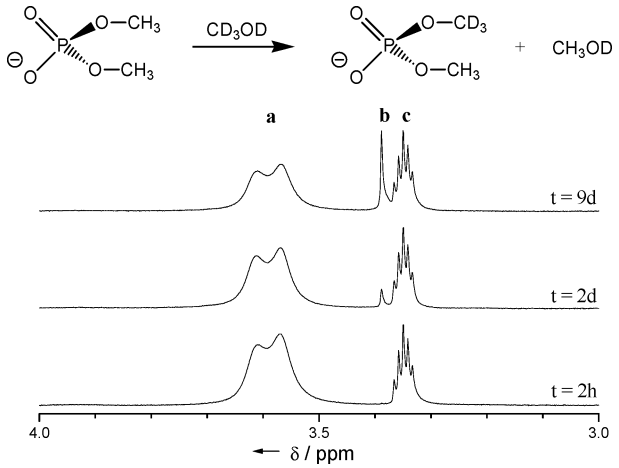

Figure 7. ^1H NMR spectra of reaction solutions containing 50 mM DMP and 2 mM **1** in D_3COD at 25 °C: (a) broad signal of $(CH_3O)_2PO_2^-$; (b) released CH_3OD at 3.39 ppm; and (c) residual CD_2HOD pentet of deuterated solvent.

Catalytic Transesterification of Dimethyl Phosphate in $\mathbf{CD_3OD}$. The activity of isolated complex **1** for the transesterification of the dimethyl phosphate (DMP) was followed by ^1H NMR spectroscopy in d_4-methanol. Reaction solutions typically contained 2 mM **1** and 50 mM sodium dimethyl phosphate. Significant broadening of the $(CH_3O)_2PO_2^-$ doublet (coupling with ^{31}P nucleus) is attributed to coordination to paramagnetic Cu(II), with rapid exchange of the phosphodiester ligand on the NMR time scale. Even at −50 °C, it was not possible to distinguish coordinated and excess "free" phosphate by NMR spectroscopy. In a D_2O solution of **1** (2 mM) and DMP (50 mM), only sharp P−OCH_3 signals are observed and DMP does obviously not coordinate to Cu. We have previously shown[20] that $\mathbf{LCu_2}$ in aqueous solution readily incorporates hydroxide even at rather low pH values <2. $(\mathbf{L})Cu_2(OH)$ does not form a DMP complex in water and is consequently not a hydrolysis catalyst, which contrasts to the behavior of $(\mathbf{L})Cu_2(OCH_3)$ in methanol.

Transesterification of DMP is followed by release of CH_3OD (Figure 7). Identity and ratio relative to DMP of reaction products $(CH_3O)(CD_3O)PO_2^-$ and $(CD_3O)_2PO_2^-$, which differ only in their isotope composition, is confirmed by mass

(22) Uchimaru, T.; Tsutzki, S.; Storer, J. W.; Tanabe, K.; Taira, K. *J. Org. Chem.* **1994**, *59*, 1835−1843.
(23) Peisach, J.; Blumberg, W. E. *Arch. Biochem. Biophys.* **1974**, *165*, 691−708.

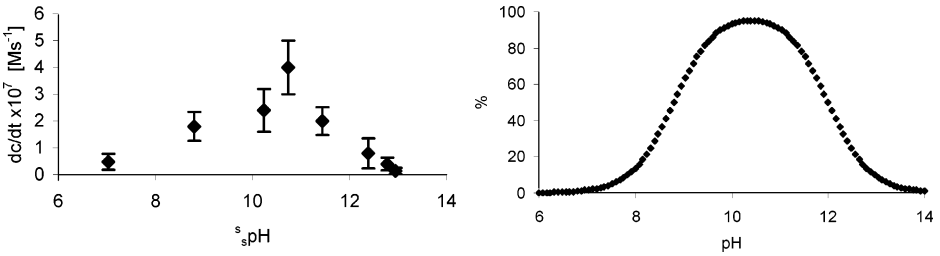

Figure 8. Left: $^{s}_{s}$pH values given in this figure were adjusted by adding methanolic stock solutions of $NaOCH_3$ or *p*-toluenesulfonic acid to **1**/NaDMP (2/50 mM) in methanol. Reactions solutions were prepared by adding the same amount of $NaOCD_3$ or *p*-toluenesulfonic acid (stock solutions in CD_3OD) to **1**/NaDMP (2/50 mM) in CD_3OD. Initial rate (d*c*/d*t*) at 55 °C of DMP cleavage in the CD_3OD reaction solution is related to the $^{s}_{s}$pH values of the corresponding CH_3OH solutions. Right: calculated pH-dependent speciation of (**L**)Cu_2(DMP)(OCH_3), % of total **LCu$_2$**, based on the first and second pK_a values 8.5 and 12 of (**L**)Cu_2(DMP).

spectrometry (LDI-MS, ESI-MS). After quantitative conversion to $(CD_3O)_2PO_2^-$ in 3 days at 55 °C, Cu^{2+} was masked by addition of aqueous Na_2CO_3, and a single ^{31}P NMR peak at 3.9 ppm (br, ^{31}P−^{2}H coupling not resolved) versus external H_3PO_4 is observed. This is consistent with a diester product ($(CH_3O)_2PO_2^-$ 4.0, $(CH_3O)PO_3^{2-}$ 7.1, $(CH_3O)_3PO$ 1.9 ppm in the same medium). These observations support a nucleophilic substitution mechanism at phosphorus with a CH_3O^- leaving group and CD_3O^- as incoming nucleophile. Experimental observations rule out an alternative pathway with nucleophilic attack of CD_3O^- at a carbon atom of DMP, which would produce the monoester $(CH_3O)PO_3^{2-}$ (not observed by mass spectrometry) and dimethyl ether-d_3 (expected at 3.2 ppm but not observed in ^{1}H NMR if the reaction is performed in a sealed NMR tube).

For reaction times <10 days at 25 °C, an approximately linear increase of methanol concentration (determined by integration of ^{1}H NMR signals) with time is observed, corresponding to 7 turnovers after 9 days without loss of catalyst activity. Cleavage rate increases linearly with concentration of catalyst **1** (1−3 mM) at a constant DMP concentration of 50 mM (Supporting Information). Because the cleavage rate is nearly the same for 10, 25, and 50 mM DMP, the **LCu$_2$** catalyst (2 mM) is saturated with substrate and we can readily calculate $k_{cat} = 9(\pm 3) \times 10^{-6}$ s^{-1} at 25 °C, the cleavage rate constant of DMP substrate bound to **LCu$_2$**. At 55 °C, k_{cat} increases to $1.2(\pm 0.5) \times 10^{-4}$ s^{-1}. In view of the hydrolytic stability of DMP, **LCu$_2$** very efficiently promotes the transesterification with a half-life of the catalyst bound DMP of about 100 min at 55 °C.

The extrapolated first-order rate constant for uncatalyzed P−O bond cleavage by hydroxide at pH 7 in water at 25 °C is in the order of 10^{-18} s^{-1}.[8a] Data for methanolysis of DMP are not available but may lie in the same range because the second-order rate constant of diphenyl phosphate cleavage by CH_3O^- is very close to the value for the hydroxide reaction in water.[17a] In control experiments, copper(II) nitrate, (2,2′-bipyridine)-$Cu(NO_3)_2$, free **L**, and the in-situ prepared mononuclear complex (**L**)$Cu(NO_3)_2$ did not cleave DMP, and no trace of methanol was detectable after 4 weeks. Cleavage of simple dialkyl phosphates by M^{2+} complexes has not been observed before. Few examples for the hydrolysis of dimethyl phosphate by strongly Lewis-acidic tri- and tetravalent metal ions have been reported, in stoichiometric reactions and often at high temperature or low pH. Examples include Co(III) ($t_{1/2}$ (DMP) = 40 days, 60 °C, pH 5.9),[24] Ce(IV) ($t_{1/2}$ (DMP) = 22 min, 60 °C, pH 1.8),[25] and Mo(IV) ($t_{1/2}$ (DMP) = 18 d, 70 °C, pH 4.0).[26]

Exploring the dependence of the DMP transesterification rate on pH was complicated by the use of deuterated methanol and elevated temperature (55 °C) to avoid very long reaction times in the kinetic assays. While the published method for pH determination using a glass electrode applies to CH_3OH and 25 °C, we are not aware of recommendations for CD_3OD and for temperature changes in this context. We therefore have attempted to compare solutions of **1** (2 mM) and NaDMP (50 mM) in CH_3OH and CD_3OD, respectively. We adjusted the $^{s}_{s}$pH in the CH_3OH medium by addition $NaOCH_3$ or *p*-toluenesulfonic acid stock solutions. We then added the same amount of $NaOCD_3$ and *p*-toluenesulfonic acid to the reaction solution in CD_3OD and measured the rate of DMP cleavage in these solutions.

Rates in CD_3OD are related to the $^{s}_{s}$pH values of corresponding CH_3OH solution in Figure 8. Included in this diagram is a pH-dependent speciation curve for (**L**)Cu_2(DMP)(OCH_3), calculated using pK_1 = 8.5 and pK_2 = 12 for the acid/base equilibria in Scheme 4. It is difficult to predict how the deuterated solvent, the elevated temperature, and the higher ionic strength affect the p*K* values and pH measurement. Note, however, that the shape of this speciation curve is similar to that of the pH-rate dependence in Figure 8. Therefore, we consider (**L**)Cu_2(DMP)(OCH_3) as the active species. The pH rate profile in Figure 8 is not consistent with either a free CD_3OD or a free CD_3O^- nucleophile. In the latter case, the rate should increase 10-fold when pH increases by one unit; even if this effect is partially compensated by a decrease in concentration of the active complex species, it cannot be fitted to the profile.

Catalytic Methanolysis of Other Phosphodiesters. To explore the influence of the alcoholate (RO^-) leaving group on catalytic rate, we have replaced DMP by various other phosphodiesters $O_2P(OR)_2^-$. Transesterification was followed by ^{1}H NMR spectroscopy, and formation of mono-transesterified products in the initial stage of the reaction was confirmed by electrospray mass spectrometry. Saturation of the catalyst was confirmed by observation of similar rate constants at 10 and 50 mM substrate concentration. Absolute and relative k_{cat} values are listed in Table 2. In phosphodiester cleavage, there is usually a strong dependence of rate constants on the pK_a of the alcohol leaving group. A linear dependence of log *k* on pK_a is observed in hydroxide cleavage,[8a] and the hydrolysis of dimethyl phosphate (extrapolated data, pK_a methanol = 15.50) is 5−6 orders of magnitude slower than that of bis(*p*-nitrophenyl)-phosphate with pK_a (nitrophenol) = 7.16. A similar factor in

(24) Kim, J. H.; Chin, J. *J. Am. Chem. Soc.* **1992**, *114*, 9792.
(25) Moss, R. A.; Ragunathan, K. G. *Chem. Commun.* **1998**, 1871−1872.
(26) Kuo, L. Y.; Barnes, L. A. *Inorg. Chem.* **1999**, *38*, 814−817.

Table 2. Absolute and Relative k_{cat} Values for Methanolysis of Phosphodiesters $O_2P(OR)(OR')^-$ Catalyzed by **1**, in Dependence on Leaving Group $-OR$[a]

–OR,–OR′	k_{cat} [s^{-1}]	relative k_{cat}
$-OCH_3$	1.2×10^{-4}	1
$-OCH_2CH_3$	1.2×10^{-6}	0.01
$-O-p\text{-}C_6H_4NO_2$	3×10^{-6}	0.025
$-OCH_2C_6H_5$	2×10^{-5}	0.17
$-OCH_3$, $-O-p\text{-}C_6H_4NO_2$	1.5×10^{-5}, 2.2×10^{-5}	0.13, 0.18

[a] CD_3OD, [**1**] = 2 mM, $[O_2P(OR)_2^-]$ = 50 mM, T = 55 °C.

Scheme 5. Proposed Mechanism for the Transesterification of $(CH_3O)_2PO_2^-$ in CD_3OD Catalyzed by **LCu₂** (**L** is omitted for clarity)

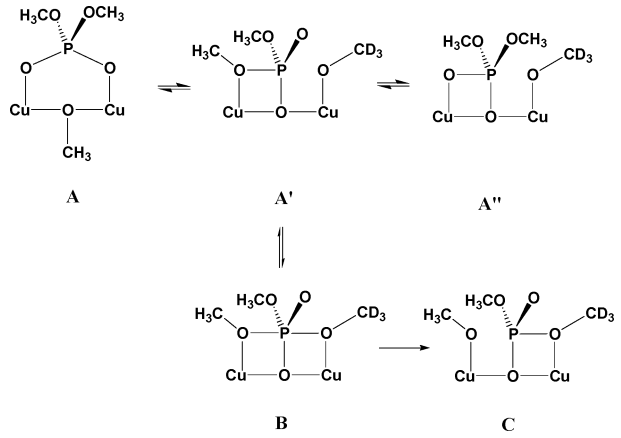

rate constant has been reported for Co(III)-promoted dimethyl phosphate and bis(*p*-nitrophenyl)phosphate hydrolysis;[8a] that is, rate accelerations by the metal are comparable for substrates with good and poor leaving groups. This trend is qualitatively confirmed by the observation that metal ions or complexes that efficiently cleave phosphodiesters with good leaving groups usually do not cleave simple dialkyl phosphates or that this reaction is too slow to be detected. Metal promoted methanolysis of phosphodiesters is less well explored, but recent studies by Brown and co-workers[17a,27] indicate that, for example, lanthanide ions are efficient promoters of aryl phosphate methanolysis or cyclophosphate ring opening, while simple −O-alkyl substitutents are not released.

In this context, the properties of transesterification catalyst **1** are rather unusual. Dimethyl phosphate and dibenzyl phosphate have similar pK_a values of the alcohol component in water (methanol, 15.50; benzyl alcohol, 15.40),[28] but dimethyl phosphate cleavage is 6 times faster. Apparently, the steric bulk of the substituent has a strong influence on methanolysis rate constant. Diethyl phosphate is even 100 times less reactive than dimethyl phosphate, possibly due to a combination of steric effects and a higher basicity of the ethoxide group (pK_a ethanol = 15.93). Surprisingly, bis(*p*-nitrophenyl)phosphate with a very good *p*-nitrophenolate leaving group due to the low pK_a of the corresponding phenol is converted at 40 times lower rate constant than dimethyl phosphate. Such an inversion of reactivity of dialkyl and diaryl phosphates has, to our knowledge, never been observed before and is attributed to a very significant influence of steric bulk at the alpha C-atom of the −OR substituent. In the substrate lithium methyl *p*-nitrophenyl phosphate, both methanolate (8 times slower than in case of DMP) and *p*-nitrophenolate (7 times faster than in case of bis(nitrophenyl)-phosphate) are released. Apparently, not only the steric effect of the leaving alcohol but also overall steric crowding in the transition state has a significant effect on catalytic rate constant. An explanation of these observations would be a transition state stabilization in phosphodiester methanolysis similar to that proposed for the Klenow fragment, including metal coordination of the alcoholate leaving group. According to molecular models, coordination of a bulky nitrophenolate leaving group (in contrast to methanolate) in phosphodiester methanolysis by **1** is disfavored by steric hindrance of nitrophenyl substitutents and CH_2 groups of the macrocycle.

Mechanistic Discussion. The mechanism of phosphodiester methanolysis catalyzed by **1** must be compatible with the following observations: very large rate enhancement for DMP methanolysis, the reactive species is $[(\mathbf{L})Cu_2(OCH_3)\{(RO)_2$-

Scheme 6. Proposed Pathway of **LCu₂** Promoted Methanolysis of Dimethyl Phosphate[a]

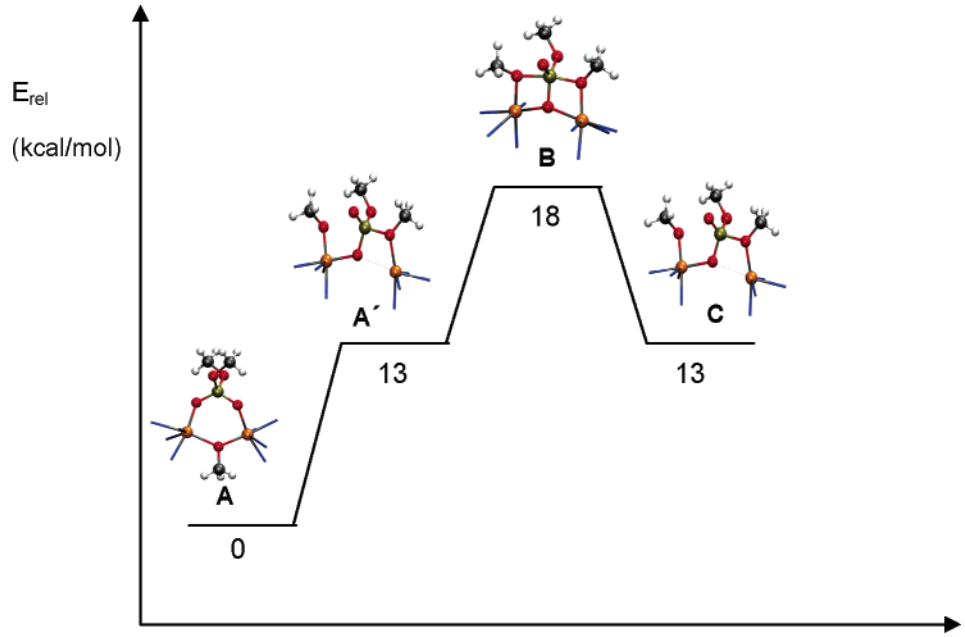

[a] Energies of intermediates (**L** is omitted for clarity) were calculated by DFT methods.

$PO_2\}]^{2+}$, and attack of external methanol or methoxide at coordinated phosphodiester is ruled out by the pH−rate-profile, and steric bulk at the α-C-atom of the leaving group −OR strongly reduces catalytic rate.

We suggest a reaction mechanism (Scheme 5) that is related to the Klenow fragment mechanism (Scheme 1), in particular with respect to the transition state stabilization.

The pK_a value of coordinated MeOH in the complex (**L**)$Cu_2(CH_3OH)$ is in the order of 6, much higher than p$K_a \approx$ 1.6 of **LCu$_2$**-coordinated water.[15] Incorporation of bridging OCH_3^- could be somewhat disfavored for steric reasons. Therefore, we suggest that the reactive complex $[(\mathbf{L})Cu_2(DMP)(OCH_3)]^{2+}$ exists in an equilibrium of an "unproductive" species **A** containing a bridging methanolate (and being structurally related to **3**) and a productive species **A′** in which bridging methanolate is replaced by a 1,1-bridging DMP. Existence of an energy-rich intermediate of a metal complex species in which a P−*O*-CH_3 group of DMP coordinates to Cu^{2+} in the ground state, related to that observed in the Klenow fragment (Scheme 1), is confirmed by DFT calculation. Moreover, species **B** was identified by DFT calculations as an intermediate rather than transition state. A reaction pathway that includes the relative DFT energies of species **A**, **A′**, and **B** is suggested in Scheme 6. Attempts to calculate the pathways including transition states between **A**, **A′**, and **B** were unsuccessful. We believe that the activation energies for the interconversion of **A** and **A′** or **A′** and **B**, respectively, are low due to the outstanding tolerance of Cu^{2+} to changes in coordinative bond distances (dynamic Jahn−Teller effect) and coordination number (5 to 6 and vice versa). As compared to the cleavage of free DMP by OH^- in water, the energy gap between ground state and trigonal-bipyramidal phosphorane intermediate reduces from 37[29] to 18 kcal/mol. Therefore, DFT calculations support the idea that the proposed mechanism accounts for the dramatic rate enhancement observed for DMP methanolysis by **1**.

Transition state (or intermediate) **B** is related to complex **4** in which **LCu$_2$** "incorporates" a transition state analogue of DMP methanolysis. Stabilization of the $-OCH_3$ leaving group by Cu^{2+} coordination would explain both the outstanding reactivity of **LCu$_2$** and the strong dependence of $O_2P(OR)_2^-$ cleavage rate on steric bulk of −OR. Chin[8a] pointed out that up to 6 orders of magnitude rate acceleration by leaving group stabilization can add up to the effects of double Lewis acid activation, generation, and positioning of metal coordinated nucleophile in dinuclear phosphoesterases. The very large rate acceleration of DMP methanolysis by **1** would be difficult to explain without a contribution of leaving group stabilization. Molecular models show that the Cu^{2+} coordination of bulky −OR leaving groups in **B** is disfavored by interference with the $N-CH_2-$py methylene groups of the ligand.

Summary

The macrocyclic dicopper(II) complex **LCu$_2$** promotes efficiently the alcoholysis of dimethyl phosphate (DMP). **LCu$_2$** is the only complex of a divalent metal ion that is capable of cleaving this highly inert substrate, and the only available catalyst for the smooth transesterification of simple dialkyl phosphates. The reactive species is the complex $[(\mathbf{L})Cu_2(DMP)(OCH_3)]^{2+}$, and a mechanism is suggested that includes double Lewis-acid activation, nucleophilic attack of coordinated OCH_3^- at P, and stabilization of the $-OCH_3$ leaving group by Cu^{2+} coordination in the transition state (intermediate, respectively).

This reaction mechanism is related to the one assumed for various phosphoryl transfer enzymes including the exonuclease subunit (Klenow fragment) of DNA polymerase I. Even if **1** is not applicable to the cleavage of biological substrates in aqueous systems, it supports the idea that cooperation of two divalent metal ions in the proposed manner might be crucial for the function of such enzymes, which often cleave phosphate esters with poor O-alkyl leaving groups.

Acknowledgment. This work was supported by the Deutsche Forschungsgemeinschaft (SFB 623).

Supporting Information Available: X-ray structural information and X-ray crystallographic files (CIF) of $[(\mathbf{L})Cu_2(NO_3)_2](NO_3)_2\cdot 2CH_3OH$ (**1**), $[(\mathbf{L})Cu_2(\mu\text{-}CO_3)(CH_3OH)](BF_4)_2\cdot 2CH_3OH$ (**2**), $[(\mathbf{L})Cu_2(1,3\text{-}\mu\text{-DMP})(NO_3)](NO_3)_2\cdot CH_3OH\cdot H_2O$ (**3**), and $[(\mathbf{L})Cu_3(\mu_3\text{-}OH)(\mu\text{-}CH_3O)_2(CH_3CN)_2](ClO_4)_3\cdot CH_3CN$ (**4**); spectrophotometric titration of **L** with Zn; dependence of initial rate of DMP cleavage on catalyst concentration; saturation kinetics for the hydrolysis of DMP by **1**; and pH titration of **1**/NaDMP (1:1) in CH_3OH. This material is available free of charge via the Internet at http://pubs.acs.org.

JA051357B

(27) Tsang, J. S. W.; Neverov, A. A.; Brown, R. S. *J. Am. Chem. Soc.* **2003**, *125*, 7602−7607.
(28) Dean, J. A. *Handbook of Organic Chemistry*; McGraw-Hill Book Co.: New York, 1987.
(29) Imhof, P.; Fischer, S.; Krämer, R.; Smith, J. C. *J. Mol. Struct. (THEOCHEM)* **2005**, *713*, 1.